# Subglacial meltwater supported aerobic marine habitats during Snowball Earth

Maxwell A. Lechte[a,b,1], Malcolm W. Wallace[a], Ashleigh van Smeerdijk Hood[a], Weiqiang Li[c], Ganqing Jiang[d], Galen P. Halverson[b], Dan Asael[e], Stephanie L. McColl[a], and Noah J. Planavsky[e]

[a]School of Earth Sciences, University of Melbourne, Parkville, VIC 3010, Australia; [b]Department of Earth and Planetary Science, McGill University, Montréal, QC, Canada H3A 0E8; [c]State Key Laboratory for Mineral Deposits Research, School of Earth Sciences and Engineering, Nanjing University, 210093 Nanjing, China; [d]Department of Geoscience, University of Nevada, Las Vegas, NV 89154; and [e]Department of Geology and Geophysics, Yale University, New Haven, CT 06511

Edited by Paul F. Hoffman, University of Victoria, Victoria, BC, Canada, and approved November 3, 2019 (received for review May 28, 2019)

**The Earth's most severe ice ages interrupted a crucial interval in eukaryotic evolution with widespread ice coverage during the Cryogenian Period (720 to 635 Ma). Aerobic eukaryotes must have survived the "Snowball Earth" glaciations, requiring the persistence of oxygenated marine habitats, yet evidence for these environments is lacking. We examine iron formations within globally distributed Cryogenian glacial successions to reconstruct the redox state of the synglacial oceans. Iron isotope ratios and cerium anomalies from a range of glaciomarine environments reveal pervasive anoxia in the ice-covered oceans but increasing oxidation with proximity to the ice shelf grounding line. We propose that the outwash of subglacial meltwater supplied oxygen to the synglacial oceans, creating glaciomarine oxygen oases. The confluence of oxygen-rich meltwater and iron-rich seawater may have provided sufficient energy to sustain chemosynthetic communities. These processes could have supplied the requisite oxygen and organic carbon source for the survival of early animals and other eukaryotic heterotrophs through these extreme glaciations.**

oxygenation | glaciation | Snowball Earth | iron formation | Fe isotopes

The Cryogenian ice ages, known as the Sturtian (717 to 660 Ma) and Marinoan (*ca*. 640 to 635 Ma) glacial episodes (1), featured low-latitude ice sheets at sea level (2–6) and widespread marine ice cover that drastically reduced the habitable ecospace for eukaryotes for millions of years. The oceans prior to these "Snowball Earth" events were characterized by oxygenated surface waters overlying a low-$O_2$ water column (7), and global ice coverage would have exacerbated oceanic anoxia. This has been suggested to have led to the mass mortality of marine aerobes (4, 5), possibly restricting aerobic eukaryotes to supraglacial environments such as low-latitude areas with partial melt on glacial surfaces or cracks in ice shelves (3, 8–10). Yet, the Cryogenian fossil record (although sparse) does not appear to have a significantly lower species richness than the preglacial interval (11), and multiple eukaryotic clades evidently endured through the ice ages (12, 13). Molecular clock and biomarker evidence may also support the persistence and diversification of key eukaryotic lineages, including metazoans, across the Cryogenian ice ages (14–17). The survival of aerobic eukaryotes through the Snowball Earth glaciations seemingly requires continually oxygenated refugia with an available organic carbon supply (12).

Geochemical and sedimentological investigation of Cryogenian synglacial sedimentary successions is essential for testing hypotheses regarding the potential habitats for aerobic eukaryotes during Snowball Earth. Although there is evidence for an oxic atmosphere (18, 19), the few geochemical studies of Cryogenian synglacial sediments are indicative of an anoxic water column during glaciation (7, 18, 20, 21). Sedimentological evidence has been used to argue for ice-free conditions during Cryogenian glaciation (e.g., ref. 22), but this evidence continues to be contentious (3) and the nature and location of potential oxic marine environments remain elusive.

Iron formations (IFs) are found in many successions deposited globally during the Sturtian glaciation (20), the first and longest Cryogenian ice age. These marine chemical sediments are unique geochemical archives of synglacial ocean chemistry. To develop a global picture of seawater redox state during extreme glaciation, we studied 9 IF-bearing Sturtian glacial successions across 3 paleocontinents (Fig. 1): Congo (Chuos Formation, Namibia), Australia (Yudnamutana Subgroup), and Laurentia (Kingston Peak Formation, United States). These IFs were selected for analysis because they are well-preserved, and their depositional environment can be reliably constrained.

## Cryogenian Glacial Environments

All 9 of the studied IF-bearing successions show sedimentological evidence for deposition in glaciomarine environments, including a stratigraphic association with ice-rafted debris-bearing marine strata and diamictites containing glacially striated clasts. Sedimentation in glaciomarine environments is controlled by distance from the grounding line where the ice shelf begins to float (23–25), and glaciomarine deposits can be broadly categorized into ice-contact, ice-proximal, and ice-distal facies (e.g., refs. 23 and 26). The ice-contact environment is a narrow setting within ~2 km of the grounding line where coarse-grained, massive diamictites are abundant due to basal ice melting and subice shelf rain-out processes (23, 26). The ice-distal environment (greater than ~10 km from the grounding line) is predominantly characterized by fine-grained, laminated sediments deposited from the settling

## Significance

**The "Snowball Earth" ice ages featured global ice sheets for millions of years, leading to oceanic anoxia and threatening the perseverance of aerobic life on Earth. Crucially, aerobic eukaryotes survived, possibly including early animals. Iron-rich chemical sediments preserved in glacial deposits offer insights into the synglacial marine redox state. We provide evidence for oxygenated waters near ice sheet grounding lines, where oxic subglacial meltwater would be supplied to the anoxic oceans. The energy released from this mixing of oxic and anoxic waters could have fueled microbial communities and sustained localized aerobic ecosystems. This meltwater oxygen pump may therefore have been critical in the survival and evolution of aerobic eukaryotes during episodes of extreme glaciation.**

Author contributions: M.A.L. and M.W.W. designed research; M.A.L., M.W.W., A.v.S.H., W.L., D.A., S.L.M., and N.J.P. performed research; M.A.L., M.W.W., A.v.S.H., W.L., D.A., and N.J.P. contributed analytic tools; M.A.L., M.W.W., A.v.S.H., W.L., G.J., G.P.H., and N.J.P. analyzed data; and M.A.L., M.W.W., and N.J.P. wrote the paper with contributions from all authors.

The authors declare no competing interest.

This article is a PNAS Direct Submission.



[1]To whom correspondence may be addressed. Email: maxwell.lechte@mail.mcgill.ca.

This article contains supporting information online at https://www.pnas.org/lookup/suppl/doi:10.1073/pnas.1909165116/-/DCSupplemental.

First published December 2, 2019.

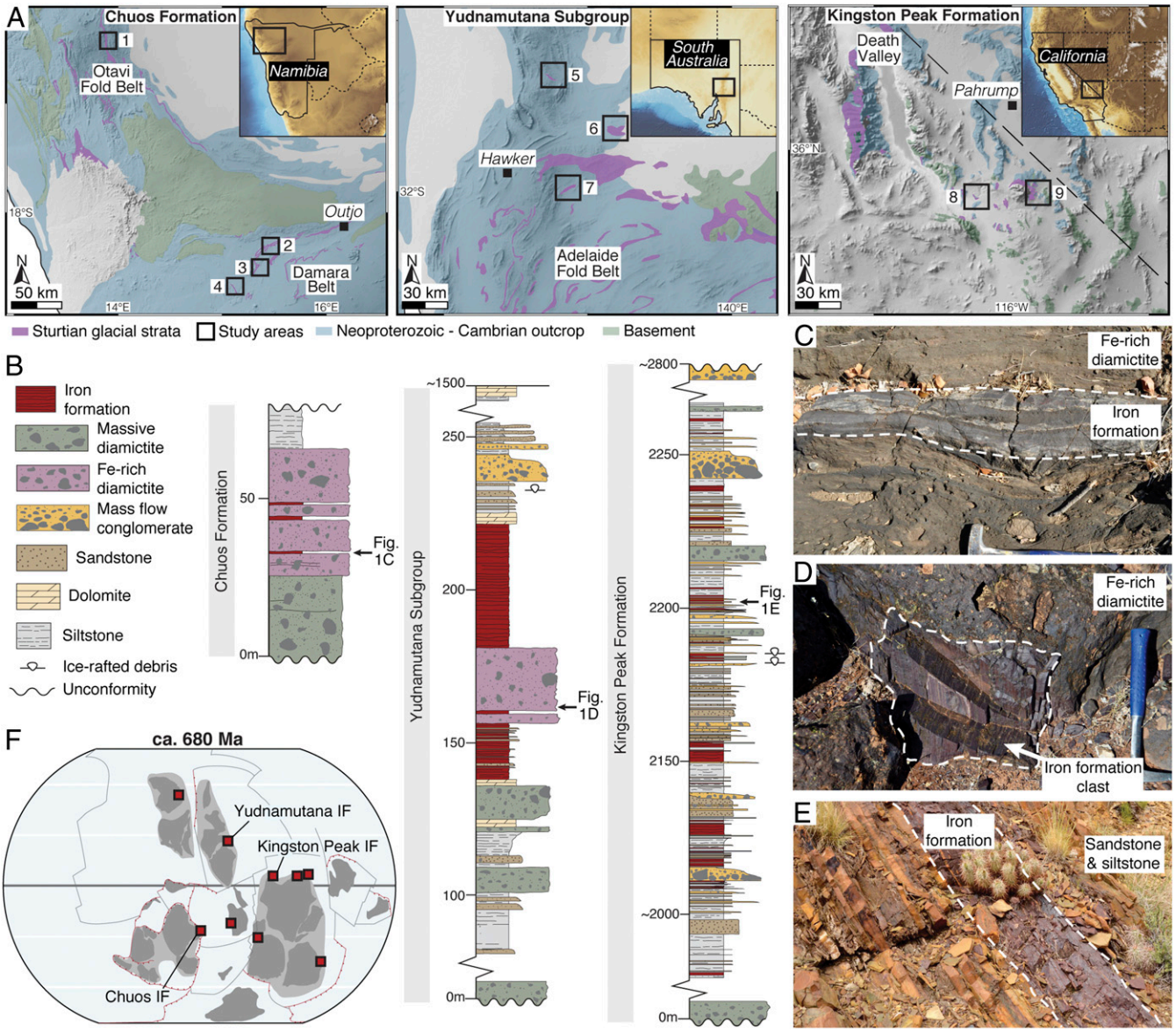


**Fig. 1.** Geological setting and sedimentology of the studied Sturtian IFs. (*A*) Geological maps of the study areas of the Chuos Formation, Kunene, Namibia (1, Okavare; 2, Landeck; 3, Lowenfontein; 4, Orusewa); the Yudnamutana Subgroup, Adelaide Fold Belt, South Australia (5, Oraparinna; 6, Willippa; 7, Holowilena South); and the Kingston Peak Formation, southern Death Valley, California (8, Sperry Wash; 9; Kingston Range). (*B*) Representative stratigraphic columns of the IF-bearing Sturtian glacial intervals of the Chuos Formation, Yudnamutana Subgroup, and Kingston Peak Formation (see *SI Appendix*, Figs. S1–S8 for stratigraphic columns from all study areas). (*C*) Interbedded diamictite and IF of the Chuos Formation, interpreted as evidence of IF deposition in an ice-contact glaciomarine environment. (*D*) Laminated IF clast within ferruginous diamictite, Yudnamutana Subgroup. (*E*) Laminated IF interbedded with siltstone and sandstone turbidites, interpreted to represent an ice-distal glaciomarine environment, Kingston Peak Formation. (*F*) Simplified global continental reconstruction at *ca*. 680 Ma highlighting the paleogeographic distribution of Sturtian IFs (red squares). The dark gray areas correspond to cratonic regions and the light gray areas represent the inferred distribution of the fragments of the supercontinent Rodinia; inferred plate boundaries and subduction zones are represented by black and red lines, respectively. Reprinted from ref. 67. Copyright (2017), with permission from Elsevier.

of suspended sediment from meltwater plumes and turbidite deposits (23, 26). The ice-proximal environment is transitional between the ice-contact and ice-distal facies. This setting features diamictites at a lower relative abundance than the ice-contact environment; these diamictites lack evidence for glaciotectonism and are interbedded with mass flow deposits and laminated marine sediments (*SI Appendix*). The depositional environments of the studied strata vary regionally and stratigraphically, and thus each IF sample was prescribed to a glaciomarine setting (ice-contact, ice-proximal, or ice-distal) based upon the predominant facies association of the interbedded lithologies.

The Sturtian glacial successions of the Chuos Formation (northern Namibia) are dominated by massive diamictites containing abundant faceted and striated clasts and in places show evidence for subglacial deformation diagnostic of the ice-contact glaciomarine environment (27, 28). The Chuos IFs are typically interbedded with these Fe-rich diamictites (Fig. 1*C*), although in some instances they are more closely associated with laminated marine sediments indicating a range of depositional environments from ice-contact to ice-distal (*SI Appendix*, Figs. S1–S3). The Sturtian Yudnamutana Subgroup (South Australia) features diamictites with outsized clasts and dropstone-bearing siltstones and shales (29). The

Yudnamutana IFs are variably associated with Fe-rich diamictites (Fig. 1*D*) and siltstones interpreted to have been deposited in all 3 glaciomarine settings (*SI Appendix*, Figs. S4–S6). The Sturtian glacial deposits of the Kingston Peak Formation (California) predominantly comprise turbiditic sandstones and siltstones, with glaciogenic debris flow conglomerates and minor diamictite (30, 31). The IFs of the Kingston Peak Formation are typically thin (<5 m) and interbedded with siltstones, sandstones, and mass flow deposits and are therefore predominantly interpreted to have been deposited in the ice-distal environment. However, rare IFs associated with massive diamictites are interpreted to be ice-proximal (Fig. 1*E* and *SI Appendix*, Figs. S7 and S8). These Sturtian IFs therefore occur in the full range of glaciomarine environments, facilitating a holistic reconstruction of the synglacial paleoredox landscape.

## Synglacial Redox Proxies

To gain insight into the paleoredox conditions of the Sturtian glaciation, we generated elemental and Fe isotope geochemical data on petrographically screened IF samples (*Materials and Methods*). These IFs are composed of fine-grained hematite with variable silica cement and low detrital content and were deposited due to the oxidation of dissolved (ferrous) Fe in seawater (e.g., refs. 20 and 28; *SI Appendix*). The IF geochemical data consistently display a well-defined trend correlating with the relative proximity to the ice-grounding line, suggestive of a paleoredox gradient (Fig. 2). The ice-contact facies IFs are the most enriched in Fe: Using Al as a proxy for detrital input, the Fe/Al ratios of ice-contact IFs are often several orders of magnitude higher than those of ice-proximal and ice-distal settings (Fig. 2*A*). The preservation of this Fe enrichment despite the high detrital sedimentation rates of ice-grounding zones (26) implies greater rates of ferrous Fe oxidation in these settings. Like Fe, Mn is a redox-sensitive metal that is soluble under anoxic conditions, forming Mn oxides in the presence of $O_2$. Mn oxides rapidly undergo reductive dissolution in the presence of ferrous Fe in seawater (32), and therefore Mn-oxide enrichments (or sedimentary Mn enrichments linked to a Mn-oxide shuttle to the sediment water interface) can be linked to an oxygenated water column (33). Only the ice-contact IFs contain appreciable Mn oxides (Fig. 2*B*), suggesting that this environment was more oxygenated during glaciation.

Redox variability in the synglacial seawater is supported by the rare earth element geochemistry of these IFs. Cerium (Ce) anomalies are a well-established, robust paleoredox proxy: Ce is depleted in seawater under oxic conditions relative to nonredox sensitive rare earth elements due to oxidative scavenging, resulting in Ce anomalies in oxic seawater ($Ce_n/Ce_n^* < 1$ when normalized to upper continental crust; *SI Appendix*). IFs are considered to reflect the rare earth element composition of their contemporaneous seawater (34), and the most prominent negative Ce anomalies are found within ice-contact IFs ($Ce_n/Ce_n^* > 0.62$; Fig. 2*C*). Therefore, these data support the interpretation that the local environment near the ice-grounding zone was oxygenated.

The Fe isotopic compositions of the studied IFs provide additional insights into Snowball Earth marine redox dynamics. The IFs have an exceptionally large range of Fe isotope ratios (Fig. 2*D*), with extremely low $\delta^{56}$Fe values down to −1.8‰ and anomalously high values up to 2.7‰. Only the ice-contact facies IFs have significant negative $\delta^{56}$Fe values (mean $\delta^{56}$Fe = −0.57‰; $n = 14$). All other Sturtian IFs have near-exclusively positive $\delta^{56}$Fe values, with ice-proximal (mean $\delta^{56}$Fe = 1.1‰; $n = 21$) and ice-distal (mean $\delta^{56}$Fe = 1.5; $n = 46$) IFs displaying a trend toward more positive values with increasing distance from the grounding line.

The Fe isotopic composition of detrital and hydrothermally sourced Fe is typically unfractionated ($-0.5 < \delta^{56}$Fe $< 0$‰), and positive $\delta^{56}$Fe values in chemical sediments provide a unique fingerprint of partial oxidation of ferrous Fe in anoxic seawater which can lead to a fractionation of ∼1 to 3‰ (35–37). After the transition to an oxidizing atmosphere during the Great Oxidation Event (*ca*. 2,400 to 2,200 Ma) upwelling ferrous Fe was typically quantitatively oxidized in the oxic, mixed ocean surface waters (32), preserving the largely unfractionated Fe isotopic signature of the ferrous Fe source. The markedly positive $\delta^{56}$Fe values of the Sturtian IFs across a range of environments, including extreme fractionations ($\delta^{56}$Fe ≤ 2.7‰) in the ice-distal IFs, represent some of the heaviest $\delta^{56}$Fe values ever reported (Fig. 2*E* and *SI Appendix*, Fig. S9). The most fractionated Fe isotope ratios reported here are comparable only to Archean values from sediments deposited prior to the advent of oxygenic photosynthesis (38). We interpret the widespread, highly positive $\delta^{56}$Fe values found in the ice-distal IFs to indicate a very small degree of ferrous Fe oxidation in an anoxic water column with severely inhibited atmospheric exchange due to widespread ice coverage (i.e., $[Fe^{2+}] > [O_2]$). These results are consistent with positive Fe isotope data reported for Cryogenian IFs from

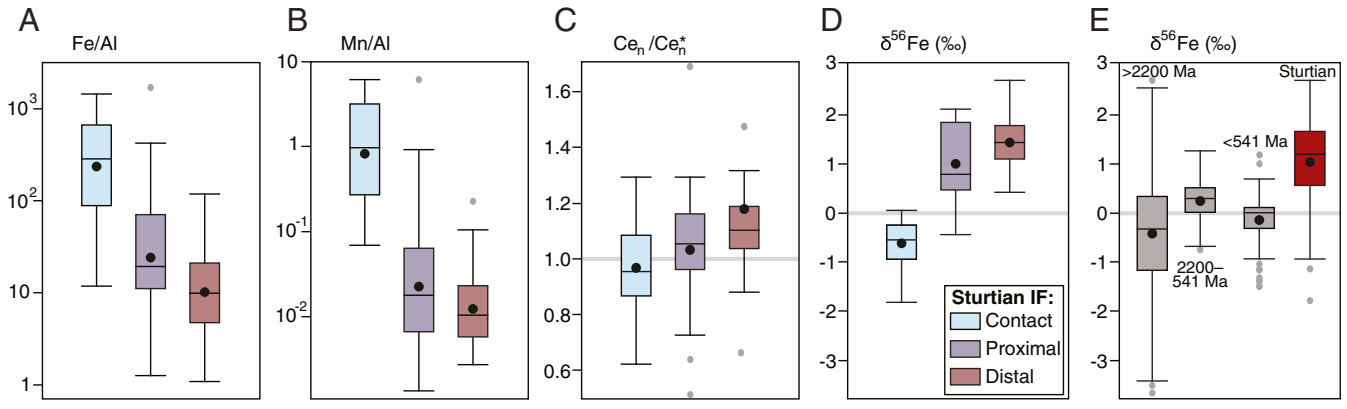


**Fig. 2.** Box plots of the Sturtian IF redox proxy data. (*A*) Fe/Al ratios, (*B*) Mn/Al ratios, (*C*) Ce anomalies ($Ce_n/Ce_n^*$), and (*D*) Fe isotope ratios ($\delta^{56}$Fe) from the ice-contact, ice-proximal, and ice-distal facies. Note that multiple facies are present in each study area (*SI Appendix*). (*E*) Box plots showing the range of Fe isotopic compositions of the Sturtian IFs (this study; $n = 81$) relative to marine sediments (IFs, shales, carbonates, hydrothermal deposits, Fe sulfides, and Fe oxides; literature data updated from ref. 68; *SI Appendix*) from 3 time bins: prior to and during the Great Oxidation Event (>2,200 Ma; $n = 1118$), between the Great Oxidation Event and the Phanerozoic (2,200 to 541 Ma; $n = 321$), and the Phanerozoic Eon (<541 Ma; $n = 252$). Boxes represent 50% of the data (the interquartile range); the mean is represented by a black circle and the median by a black line. Outliers (outside the interquartile range) are represented by a gray circle; extreme outliers (greater than double the interquartile range from the median; $n = 6$) are not shown. Whiskers represent extreme values that are not outliers.

southern China (39–41), northern Canada (42), and Australia and Alaska (43). Collectively, these data show anoxic seawater dominated the synglacial Sturtian oceans.

Negative seawater $\delta^{56}$Fe values can result from distillation during the progressive oxidation of a ferrous Fe reservoir (35), and these Fe isotopic characteristics can be transferred to the sediment pile through local quantitative ferrous Fe oxidation (*SI Appendix*). The highly fractionated ice-contact IFs show the most negative $\delta^{56}$Fe values ($\delta^{56}Fe \geq -1.8‰$) reported for rocks deposited after the Great Oxidation Event (*SI Appendix*, Fig. S9). We interpret these negative $\delta^{56}$Fe values to reflect extensive oxidation of a highly evolved ferrous Fe reservoir proximal to the grounding line. This model is consistent with the common occurrence of markedly positive $\delta^{56}$Fe values in most Sturtian IFs. Therefore, these geochemical data demonstrate a relatively high degree of oxygenation in the ice-contact glaciomarine environment but widespread marine anoxia distal from glaciated margins, providing direct evidence for environment-specific marine oxygenation during Snowball Earth.

## Glacial Meltwater Oxygen Pump

Several independent geochemical indicators (redox-sensitive metal enrichments, Ce anomalies, and Fe isotopic compositions) in Sturtian glacial successions display the same trend of increasing seawater oxygenation with proximity to the ice sheet. The interpretation that the ice-contact environment is significantly more oxidizing than other marine environments is supported by statistical analyses (*SI Appendix*, Fig. S10). We interpret this paleoredox gradient as strong evidence for a glacially derived $O_2$ source. Glacial ice formed via the accumulation and compaction of snow (meteoric ice) contains trapped air bubbles and constitutes the majority of the mass of modern ice sheets. Glacial meltwater can be produced on the ice sheet surface, at the base of ice shelves, and at the ice sheet base (due to geothermal flux, pressure, and frictional heating). The melting of meteoric ice by any of these processes typically produces meltwater containing $O_2$ dissolved from trapped air bubbles (44). This meltwater supplies subglacial systems with $O_2$ (45), as seen in modern subglacial lakes that are oxygenated due to meltwater supply (46).

Glacial hydrology and thermal regime influence the redox state of subglacial meltwater: When residence time is high due to inefficient drainage, subglacial meltwater $O_2$ can be consumed due to prolonged water–rock interactions and microbial activity (45, 47). Conversely, when meltwater drainage is efficient, oxygenated meltwater can be delivered to ice shelf waters (48). The sedimentology of the studied Cryogenian glacial successions—featuring thick diamictite successions with abundant clasts of diverse lithologies, dropstones, channel structures, glaciotectonized strata, and evidence of ice sheet dynamism—is consistent with deposition beneath extensive ice shelves fed by ice streams from polythermal ice sheets (*SI Appendix*). In this scenario, subglacial meltwater would likely be supplied to the proglacial setting by an interconnected, channelized drainage system and supplemented by basal melting of the ice shelf. Oxygen oases may therefore have been localized to the outlets of ice streams where meltwater supply was sufficient to maintain oxygenated glaciomarine habitats.

The basal melting of meteoric glacial ice to generate oxygenated meltwater, and the subsequent oxidation of ferruginous seawater in the subice shelf environment (49, 50), provide a simple explanation for the IF geochemical trends (Fig. 3) as well as the localized association between IFs and glacial deposits during this time. Although Sturtian IFs have previously been assumed to represent oxidation during deglaciation (5), we suggest that these deposits instead point to a unique redox environment in the synglacial oceans. IFs in glacial sediments are a "red flag" for marine oxidation processes, and this association is most apparent during the Sturtian glaciation (*SI Appendix*), which likely featured a strong redox contrast between an oxygenated atmosphere and ferrous Fe-rich oceans

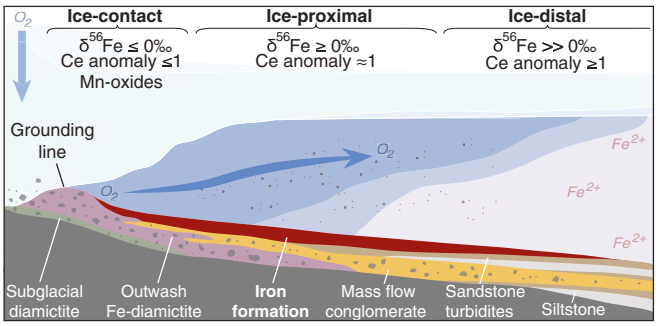


**Fig. 3.** Schematic model for the outwash of oxygenated basal meltwater to anoxic glaciomarine environments (not to scale). IFs deposited in ice-contact settings (within ~2 km of the grounding line) are characterized by negative $\delta^{56}$Fe values and may feature negative Ce anomalies and Mn-oxide enrichment, indicative of oxidizing conditions. Ice-proximal IFs (~2 to 10 km from the grounding line) display predominantly positive $\delta^{56}$Fe values and negligible to slight positive Ce anomalies. Ice-distal IFs (greater than ~10 km from the grounding line) feature slight positive Ce anomalies and highly positive $\delta^{56}$Fe values, with negligible Mn oxides. These geochemical trends are indicative of oxygenated glaciomarine environments which could have supported aerobic eukaryotes despite widespread anoxia during extreme glaciation. Microaerophilic Fe-oxidizing bacteria may have proliferated where $O_2$-bearing meltwater mixed with ferruginous seawater, potentially supporting heterotrophic food webs.

fostered by ice cover. Although atmospheric $pO_2$ estimates vary, an oxidizing atmosphere is considered to have been maintained during Snowball Earth (18, 19), an assertion supported by these data. Ongoing oxygenic photosynthesis is required to sustain an oxygenated atmosphere throughout a Snowball Earth event in order to balance the outgassing of reduced volcanic gases (51). We suggest that these deposits are evidence for ongoing photosynthetic activity which must have continued in surficial environments throughout the glaciation (3, 9).

## Oxygenated Marine Ecosystems

The fossil record indicates that multiple extant eukaryotic clades had evolved prior to the Sturtian glaciation, including archaeplastidans, opisthokonts, and amoebozoans (11, 13, 52), and several other eukaryotic lineages are thought to have emerged before the Cryogenian (15, 16, 53). Many of these eukaryotes are obligate aerobes, and therefore the oxygenation of the Cryogenian glaciated margins by a glacial meltwater pump may have been critical for maintaining synglacial ecosystems. Basal melting would have maintained a consistent background supply of meltwater to proglacial marine environments during the Cryogenian glaciations (3, 54). By analogy to the modern glaciated margins of Antarctica, plumes of meltwater could have extended for multiple kilometers from the grounding line (e.g., ref. 55), surrounding the paleocoastline of the rifting Rodinia supercontinent (Fig. 1*F*) and providing a stable redox environment for aerobic eukaryotes. Thus, these oxygenated habitats would likely have been more extensive and more stable over multimillion-year timescales than other hypothesized oases such as ice crevasses. If ice-free polynyas existed, the currently available geochemical evidence for pervasive anoxia suggests that they were not widespread or stable throughout the Sturtian glaciation. Glaciomarine settings would therefore have been important oxygenated refugia for a range of protists.

Given that the availability of $O_2$ is vital for complex multicellular life (56), subice shelf oxygen oases may have also been important refugia for early animals. Most current molecular clock analyses estimate that animal multicellularity evolved prior to the Cryogenian (e.g., refs. 15 and 16; *SI Appendix*). The earliest animals were likely benthic, as sponges are considered to be a basal metazoan clade (e.g., refs. 15 and 16), and we suggest that the

oxygenation of the seafloor in glaciomarine environments could have provided a habitat for possible Cryogenian benthic macrofauna. Freshwater inputs could have also been important for maintaining a lower ambient salinity for early sponges, as ice sheet growth would have raised the salinity of the synglacial oceans during glacial onset. Modern sponges can be abundant and diverse in schizohaline and hypersaline marine environments. However, the taxonomic relationships of euryhaline sponges, and the mechanisms responsible for hypersalinity tolerance, are unresolved (57, 58). Therefore, it remains unclear whether early sponges would have been capable of osmoregulation (9). If sponges survived Snowball Earth, then basal melting may have helped to establish suitable habitats for early metazoans in glaciomarine environments.

These glaciomarine environments may have had similarities to modern Antarctic subice shelf settings, where diverse ecosystems of animals (including sponges) and other heterotrophic eukaryotes thrive under hundreds of meters of ice (59, 60). The chemical weathering of subglacial rock leads to delivery of bioessential nutrients to glaciomarine habitats via subglacial meltwaters (61). Although this process also supplies organic carbon sourced from subglacial microbial assemblages (62), the extent of ice coverage during Snowball Earth would have likely restricted photosynthetic primary productivity and food sources may have been comparatively scarce in the Cryogenian synglacial oceans. However, photosynthetic refugia would have supplied dissolved and particulate organic matter to the synglacial oceans. Supraglacial melting, and subsequent meltwater draining through moulin networks, could have transported organic matter from surface environments (such as cryoconite pans; refs. 8 and 9) to subice shelf settings.

Primary productivity driven by chemoautotrophic bacteria may have also been an important source of labile organic matter to Cryogenian glaciomarine habitats. Chemoautotrophic activity maintains diverse heterotrophic ecosystems in modern oxic subglacial lakes (46, 63). Similarly, chemosynthesis in modern subice shelf environments fosters metazoan communities up to 100 km from the open ocean (64, 65), where the advection of photosynthetically derived organic carbon is considered to be negligible (60). Planktonic marine Fe-oxidizing bacteria are widespread in aqueous environments where $O_2$ and ferrous Fe coexist (e.g., ref. 66). An oxygen gradient established by the confluence of plumes of $O_2$-bearing meltwater with ferrous Fe-rich seawater would have produced ideal conditions for the proliferation of microaerophilic Fe-oxidizing bacteria during Snowball Earth. Planktonic marine Fe-oxidizing bacteria shed their precipitated Fe-oxides (66): this process may have contributed to IF deposition and would have permitted the remineralization of produced organic carbon. Chemosynthesizers may therefore have been an important constituent of heterotrophic food webs during Snowball Earth.

## Conclusions

IFs preserved within Sturtian glacial successions provide valuable insights into the effects of global glaciation on ocean chemistry. Our observations bolster the case that there was widespread marine anoxia during the most severe ice age in Earth's history, supportive of significant ice coverage inhibiting exchange between the oceans and the oxic atmosphere. This oceanic anoxia would have restricted marine habitats for aerobic eukaryotes. However, Cryogenian IFs provide empirical evidence for oxygenated glaciomarine habitats during Snowball Earth. We suggest that atmospheric oxygen was transferred to the oceans throughout the Sturtian glaciation via a glacial "oxygen pump," whereby outwash of subglacial meltwater ventilated glaciomarine environments near the ice-shelf grounding line. These subice shelf oxygen oases likely fostered chemosynthetic and heterotrophic ecosystems, aiding the survival and shaping the subsequent radiation of key lineages of aerobic eukaryotes through extreme glaciation.

## Materials and Methods

IF samples were prepared as polished thin sections and petrographically analyzed using reflected light microscopy and scanning electron microscopy. Well-preserved samples were crushed to a fine powder using an agate ring mill. For bulk rock major element analyses, sample powders ($n = 89$) were prepared as fused glass discs and analyzed using X-ray fluorescence. Sample powder splits ($n = 111$) were also digested for bulk rock elemental analyses using an inductively coupled plasma mass spectrometer (ICP-MS). For $\delta^{56}$Fe measurements ($n = 81$), Fe was purified using ion-exchange chromatography and measured using a multicollector ICP-MS. For in situ geochemical analyses ($n = 93$), rare earth element contents were measured using laser ablation ICP-MS. Refer to *SI Appendix, Supplementary Materials and Methods* for detailed methods.

**Data Availability.** All data discussed in the paper are included in Dataset S1.

**ACKNOWLEDGMENTS.** We thank A. Greig, P. Schreck, G. Hutchinson, and B. O'Connell for laboratory assistance; A. Shuster for field assistance; and A. Prave, D. Le Heron, and K. Hoffmann for locality advice. This work was supported by funding from the Australian Government Research Training Program Scholarship and Albert Shimmins Award to M.A.L.; Australian Research Council Discovery Grant DP130102240 to M.W.W.; and NASA Astrobiology Postdoctoral Fellowship, Puzey Fellowship, and Australian Research Council Discovery Early Career Researcher Award (DE190100988) to A.v.S.H. N.J.P. acknowledges support from the NASA Astrobiology Institute under Cooperative Agreement NNA15BB03A, issued through the Science Mission Directorate. We thank the handling editor and 2 reviewers for their constructive feedback.

1. A. D. Rooney, J. V. Strauss, A. D. Brandon, F. A. Macdonald, A Cryogenian chronology: Two long-lasting synchronous Neoproterozoic glaciations. *Geology* **43**, 459–462 (2015).
2. W. Harland, "Evidence of Late Precambrian glaciation and its significance" in *Problems in Palaeoclimatology*, A. E. M. Nairn, Ed. (Interscience, London, 1964), vol. 705, pp. 119–149.
3. P. F. Hoffman *et al*., Snowball Earth climate dynamics and Cryogenian geology-geobiology. *Sci. Adv.* **3**, e1600983 (2017).
4. P. F. Hoffman, A. J. Kaufman, G. P. Halverson, D. P. Schrag, A neoproterozoic snowball earth. *Science* **281**, 1342–1346 (1998).
5. J. L. Kirschvink, "Late Proterozoic low-latitude global glaciation: The Snowball Earth" in *The Proterozoic Biosphere : A Multidisciplinary Study* (Cambridge University Press, New York, 1992), pp. 51–52.
6. D. A. Evans, Stratigraphic, geochronological, and paleomagnetic constraints upon the Neoproterozoic climatic paradox. *Am. J. Sci.* **300**, 347–433 (2000).
7. E. A. Sperling *et al*., Statistical analysis of iron geochemical data suggests limited late Proterozoic oxygenation. *Nature* **523**, 451–454 (2015).
8. W. F. Vincent *et al*., Ice shelf microbial ecosystems in the high arctic and implications for life on snowball earth. *Naturwissenschaften* **87**, 137–141 (2000).
9. P. F. Hoffman, Cryoconite pans on snowball earth: Supraglacial oases for Cryogenian eukaryotes? *Geobiology* **14**, 531–542 (2016).
10. I. Hawes, A. D. Jungblut, E. D. Matys, R. E. Summons, The "Dirty Ice" of the McMurdo Ice Shelf: Analogues for biological oases during the Cryogenian. *Geobiology* **16**, 369–377 (2018).
11. L. A. Riedman, P. M. Sadler, Global species richness record and biostratigraphic potential of early to middle Neoproterozoic eukaryote fossils. *Precambrian Res.* **319**, 6–18 (2017).
12. M. Moczydłowska, The Ediacaran microbiota and the survival of Snowball Earth conditions. *Precambrian Res.* **167**, 1–15 (2008).
13. P. A. Cohen, F. A. Macdonald, The Proterozoic record of eukaryotes. *Paleobiology* **41**, 610–632 (2015).
14. J. A. Zumberge *et al*., Demosponge steroid biomarker 26-methylstigmastane provides evidence for Neoproterozoic animals. *Nat. Ecol. Evol.* **2**, 1709–1714 (2018).
15. M. Dohrmann, G. Wörheide, Dating early animal evolution using phylogenomic data. *Sci. Rep.* **7**, 3599 (2017).
16. D. H. Erwin *et al*., The Cambrian conundrum: early divergence and later ecological success in the early history of animals. *Science* **334**, 1091–1097 (2011).
17. J. J. Brocks *et al*., The rise of algae in Cryogenian oceans and the emergence of animals. *Nature* **548**, 578–581 (2017).
18. B. W. Johnson, S. W. Poulton, C. Goldblatt, Marine oxygen production and open water supported an active nitrogen cycle during the Marinoan Snowball Earth. *Nat. Commun.* **8**, 1316 (2017).
19. W. Wei *et al*., Redox condition in the Nanhua Basin during the waning of the Sturtian glaciation: A chromium-isotope perspective. *Precambrian Res.* **319**, 198–210 (2018).
20. G. M. Cox *et al*., Neoproterozoic iron formation: An evaluation of its temporal, environmental and tectonic significance. *Chem. Geol.* **362**, 232–249 (2013).
21. S. Gu, Y. Fu, J. Long, Predominantly Ferruginous Conditions in South China during the Marinoan Glaciation: Insight from REE Geochemistry of the Syn-glacial Dolostone from the Nantuo Formation in Guizhou Province, China. *Minerals* **9**, 348 (2019).
22. P. A. Allen, J. L. Etienne, Sedimentary challenge to snowball Earth. *Nat. Geosci.* **1**, 817–825 (2008).

23. J. Evans, C. Pudsey, Sedimentation associated with Antarctic Peninsula ice shelves: Implications for palaeoenvironmental reconstructions of glacimarine sediments. *J. Geol. Soc. London* **159**, 233–237 (2002).
24. E. W. Domack, P. T. Harris, A new depositional model for ice shelves, based upon sediment cores from the Ross Sea and the Mac. Robertson shelf, Antarctica. *Ann. Glaciol.* **27**, 281–284 (1998).
25. M. J. Hambrey, N. F. Glasser, Discriminating glacier thermal and dynamic regimes in the sedimentary record. *Sediment. Geol.* **251**, 1–33 (2012).
26. K. Brodzikowski, A. Van Loon, A systematic classification of glacial and periglacial environments, facies and deposits. *Earth Sci. Rev.* **24**, 297–381 (1987).
27. M. E. Busfield, D. P. Le Heron, Glacitectonic deformation in the Chuos Formation of northern Namibia: implications for Neoproterozoic ice dynamics. *Proc. Geol. Assoc.* **124**, 778–789 (2013).
28. M. Lechte, M. Wallace, Sub–ice shelf ironstone deposition during the Neoproterozoic Sturtian glaciation. *Geology* **44**, 891–894 (2016).
29. D. P. Le Heron, G. Cox, A. Trundley, A. S. Collins, Two Cryogenian glacial successions compared: Aspects of the Sturt and Elatina sediment records of South Australia. *Precambrian Res.* **186**, 147–168 (2011).
30. D. P. Le Heron, M. E. Busfield, A. R. Prave, Neoproterozoic ice sheets and olistoliths: Multiple glacial cycles in the Kingston Peak Formation, California. *J. Geol. Soc. London* **171**, 525–538 (2014).
31. M. A. Lechte, M. W. Wallace, A. van Smeerdijk Hood, N. Planavsky, Cryogenian iron formations in the glaciogenic Kingston Peak Formation, California. *Precambrian Res.* **310**, 443–462 (2018).
32. V. Busigny *et al*., Iron isotopes in an Archean ocean analogue. *Geochim. Cosmochim. Acta* **133**, 443–462 (2014).
33. N. J. Planavsky *et al*., Evidence for oxygenic photosynthesis half a billion years before the Great Oxidation Event. *Nat. Geosci.* **7**, 283 (2014).
34. N. Planavsky *et al*., Rare earth element and yttrium compositions of Archean and Paleoproterozoic Fe formations revisited: New perspectives on the significance and mechanisms of deposition. *Geochim. Cosmochim. Acta* **74**, 6387–6405 (2010).
35. O. J. Rouxel, A. Bekker, K. J. Edwards, Iron isotope constraints on the Archean and Paleoproterozoic ocean redox state. *Science* **307**, 1088–1091 (2005).
36. N. Dauphas *et al*., Clues from Fe isotope variations on the origin of early Archean BIFs from Greenland. *Science* **306**, 2077–2080 (2004).
37. L. Wu, B. L. Beard, E. E. Roden, C. M. Johnson, Stable iron isotope fractionation between aqueous Fe(II) and hydrous ferric oxide. *Environ. Sci. Technol.* **45**, 1847–1852 (2011).
38. W. Li *et al*., An anoxic, Fe (II)-rich, U-poor ocean 3.46 billion years ago. *Geochim. Cosmochim. Acta* **120**, 65–79 (2013).
39. B. Yan, X. Zhu, S. Tang, M. Zhu, Fe isotopic characteristics of the Neoproterozoic BIF in Guangxi Province and its implications. *Acta Geol. Sin.* **84**, 1080–1086 (2010).
40. V. Busigny *et al*., Origin of the Neoproterozoic Fulu iron formation, South China: Insights from iron isotopes and rare earth element patterns. *Geochim. Cosmochim. Acta.* **242**, 123–142 (2018).
41. X.-K. Zhu, J. Sun, Z.-H. Li, Iron isotopic variations of the Cryogenian banded iron formations: A new model. *Precambrian Res.* **331**, 105359 (2019).
42. G. P. Halverson *et al*., Fe isotope and trace element geochemistry of the Neoproterozoic syn-glacial Rapitan iron formation. *Earth Planet. Sci. Lett.* **309**, 100–112 (2011).
43. G. M. Cox *et al*., A model for Cryogenian iron formation. *Earth Planet. Sci. Lett.* **433**, 280–292 (2016).
44. G. Brown, M. Tranter, M. Sharp, T. Davies, S. Tsiouris, Dissolved oxygen variations in Alpine glacial meltwaters. *Earth Surf. Process. Landf.* **19**, 247–253 (1994).
45. M. Tranter, M. Skidmore, J. Wadham, Hydrological controls on microbial communities in subglacial environments. *Hydrol. Process. Int. J.* **19**, 995–998 (2005).
46. B. C. Christner *et al*.; WISSARD Science Team, A microbial ecosystem beneath the West Antarctic ice sheet. *Nature* **512**, 310–313 (2014). Erratum in: *Nature* **514**, 394 (2014).
47. J. A. Mikucki *et al*., A contemporary microbially maintained subglacial ferrous "ocean". *Science* **324**, 397–400 (2009).
48. A. Jenkins, The impact of melting ice on ocean waters. *J. Phys. Oceanogr.* **29**, 2370–2381 (1999).
49. P. F. Hoffman, 28th DeBeers Alex. Du Toit Memorial Lecture, 2004. On Cryogenian (Neoproterozoic) ice-sheet dynamics and the limitations of the glacial sedimentary record. *S. Afr. J. Geol.* **108**, 557–577 (2005).
50. P. F. Hoffman, F. A. Macdonald, G. P. Halverson, "Chemical sediments associated with Neoproterozoic glaciation: iron formation, cap carbonate, barite and phosphorite" in *The Geological Record of Neoproterozoic Glaciations*, E. Arnaud, G. P. Halverson, G. Shields-Zhou, Eds. (Geological Society of London, 2011), vol. 36, pp. 67–80.
51. T. A. Laakso, D. P. Schrag, A theory of atmospheric oxygen. *Geobiology* **15**, 366–384 (2017).
52. C. C. Loron *et al*., Early fungi from the Proterozoic era in Arctic Canada. *Nature* **570**, 232–235 (2019). Correction in: *Nature* **571**, E11 (2019).
53. L. Eme, S. C. Sharpe, M. W. Brown, A. J. Roger, On the age of eukaryotes: Evaluating evidence from fossils and molecular clocks. *Cold Spring Harb. Perspect. Biol.* **6**, a016139 (2014).
54. Y. Ashkenazy *et al*., Dynamics of a snowball earth ocean. *Nature* **495**, 90–93 (2013).
55. H. M. Dierssen, R. C. Smith, M. Vernet, Glacial meltwater dynamics in coastal waters west of the Antarctic peninsula. *Proc. Natl. Acad. Sci. U.S.A.* **99**, 1790–1795 (2002).
56. D. C. Catling, C. R. Glein, K. J. Zahnle, C. P. McKay, Why O2 is required by complex life on habitable planets and the concept of planetary "oxygenation time". *Astrobiology* **5**, 415–438 (2005).
57. K. Rützler, S. Duran, C. Piantoni, Adaptation of reef and mangrove sponges to stress: Evidence for ecological speciation exemplified by Chondrilla caribensis new species (Demospongiae, Chondrosida). *Mar. Ecol. (Berl.)* **28**, 95–111 (2007).
58. A. Pisera, K. Rützler, J. Kaz'mierczak, S. Kempe, Sponges in an extreme environment: suberitids from the quasi-marine Satonda Island crater lake (Sumbawa, Indonesia). *J. Mar. Biol. Assoc. U. K.* **90**, 203–212 (2010).
59. M. Riddle, M. Craven, P. Goldsworthy, F. Carsey, A diverse benthic assemblage 100 km from open water under the Amery Ice Shelf, Antarctica. *Paleoceanography* **22**, PA1204 (2007).
60. S. Kim, Complex life under the McMurdo Ice Shelf, and some speculations on food webs. *Antarct. Sci.* **31**, 1–9 (2019).
61. J. Wadham *et al*., The potential role of the Antarctic Ice Sheet in global biogeochemical cycles. *Earth Environ. Sci. Trans. R. Soc. Edinburgh* **104**, 55–67 (2013).
62. K. A. Cameron *et al*., Meltwater export of prokaryotic cells from the Greenland ice sheet. *Environ. Microbiol.* **19**, 524–534 (2017).
63. J. A. Mikucki *et al*.; WISSARD Science Team, Subglacial Lake Whillans microbial biogeochemistry: A synthesis of current knowledge. *Philos Trans A Math Phys Eng Sci* **374**, 20140290 (2016).
64. S. G. Horrigan, Primary production under the Ross Ice Shelf, Antarctica 1. *Limnol. Oceanogr.* **26**, 378–382 (1981).
65. E. Domack *et al*., A chemotrophic ecosystem found beneath Antarctic ice shelf. *Eos (Wash. D.C.)* **86**, 269–272 (2005).
66. E. K. Field *et al*., Planktonic marine iron oxidizers drive iron mineralization under low-oxygen conditions. *Geobiology* **14**, 499–508 (2016).
67. A. S. Merdith *et al*., A full-plate global reconstruction of the Neoproterozoic. *Gondwana Res.* **50**, 84–134 (2017).
68. V. E. McCoy, D. Asael, N. Planavsky, Benthic iron cycling in a high-oxygen environment: Implications for interpreting the Archean sedimentary iron isotope record. *Geobiology* **15**, 619–627 (2017).